Hydrogels Combined with Silver Nanoparticles against Antimicrobial Resistance

Subjects: Chemistry, Medicinal | Medicine, Research & Experimental | Chemistry, Applied

Contributor: Yolice Patricia Moreno Ruiz, Luís André de Almeida Campos, Maria Andressa Alves Agreles, André Galembeck, Isabella Macário Ferro Cavalcanti

The development of multidrug-resistant (MDR) microorganisms has increased dramatically as a natural consequence of the misuse and overuse of antimicrobials. The World Health Organization (WHO) recognizes that this is one of the top ten global public health threats facing humanity today, demanding urgent multisectoral action. In this sense, metallic nanoparticles (such as silver nanoparticles) have emerged as promising alternatives due to their outstanding antibacterial and antibiofilm properties. The efficient delivery of the nanoparticles (NPs) is also a matter of concern, and studies have demonstrated that hydrogels present an excellent ability to perform this task.

Keywords: antibiotic resistance ; hydrogel ; bacterial ; antibiofilm

1. Silver Nanoparticles (Ag NPs)

Silver (Ag) nanoparticles (NPs) can damage the extracellular membrane of bacteria and their intracellular components, exhibiting a broad-spectrum antimicrobial effect [1]. Many Ag NP synthesis strategies have been developed to allow specific Ag NP surface properties, which, in turn, strongly depend on the characteristics of the reducing agent and the type of stabilizer used during their synthesis [1][2][3][4][5][6][7][8].

According to Sondi et al. [9], Ag NPs can cause harm to *E. coli* by forming pits in the cell wall, which could increase its permeability and affect the membrane vesicles. Such damage has also been observed in other bacteria, such as *Scrub typhus*, *P. aeruginosa*, and *Vibrio cholerae* [10], which is attributed to the ability of Ag NPs to interact with some of its components, such as lipopolysaccharides (LPSs), and phosphatidylethanolamines (PEs) [11].

Mirzajani et al. [12] suggested that the ability of Ag NPs to harm the bacterial cell wall may result from their interaction with the peptidoglycan layer, since Ag NPs attack the β-1-4 bonds of N-acetylglucosamine and N-acetylmuramic acid of the glycan chain in the cell membrane of *S. aureus*. Additionally, Ag NPs may produce free radicals, such as reactive oxygen species (ROS), inside and outside the bacteria [13][14]. Elevated ROS levels are known to damage cell DNA, proteins, and enzymes, which could, in turn, interfere with the normal metabolism of bacteria [15]. It was found that Ag^+ ions released from Ag NPs can damage bacterial membrane function. In particular, the differences in Ag^+ concentration can induce a difference between the pH and the electrical potential inside and outside the membrane vesicles in *Vibro cholerae*, leading to the failure of membrane respiration and H^+ leakage [16].

The effect of Ag NPs on the bacterial membrane is related to their physicochemical properties, such as size, shape, surface area, surface charge, oxidation state, and surface chemistry. It has been reported that Ag NPs with small size and colloidal stability are preferred rather than those susceptible to aggregation [1][2][17][18][19][20]. The size of NPs is one of the most critical aspects determining their interaction with cells. Actually, Ag NP interaction is size-dependent [10][21]. Several works have shown that Ag NPs with a diameter of 3–10 nm, are the most effective in killing bacteria due to their preferential direct interaction with the bacterial membrane [22] and how fast the bacterial killing took place after their interaction [21].

The shape of Ag NPs can directly influence the available contact area needed to facilitate interactions of Ag NPs with the bacterial membrane. A comparative study using polyvinylpyrrolidone (PVP)-coated Ag NPs with different shapes suggested a strong correlation between the shape of the Ag NPs and their bactericidal properties. For example, Ag nanoplates (two-dimensional structure, 2D) showed the highest antimicrobial activity against *S. aureus* and *E. coli*, when compared to Ag nanorods (one-dimensional structure, 1D) and spherical Ag NPs (zero-dimensional structure, 0D). Sadeghi et al. [23] showed that Ag nanoplates exhibited the largest surface area, providing the most significant contact area to interact with the bacterial cell wall.

The Ag NP surface charge is also important. It was observed that positively charged Ag NPs using capping agents such as poly(amide amine) dendrimers (PAMAM) [24], poly(ethyleneimine) (PEI) [25], poly(ethylene glycol) (PEG), and polyvinylpyrrolidone (PVP) [26] facilitated the interaction between the particles and the negatively charged bacterial membrane [24]. Ag NPs with a negative surface charge have shown lower antimicrobial activity [27] due to the strong

repulsion between the particles and the bacterial wall. This limits the interaction between Ag NPs and bacteria and considerably weakens their antimicrobial effect.

Ag NPs have been also combined with antibiotics (ampicillin, amoxicillin, chloramphenicol, erythromycin, among others) [28] by chelation of the active groups. The combination of Ag NPs with other materials, such as polycationic chitosan, has shown promising results by facilitating the attachment of Ag NPs to the negatively charged bacterial wall [29]. Mishra et al. [30] developed a multifunctional system of Ag NPs embedded in the chitosan-polyethylene glycol (CS-PEG) hydrogel. This implantable device inhibited biofilm formation and the released the drug payload at the same time. Chen et al. [31] prepared a chitosan sponge containing Ag NPs and used it as a tissue for wound healing. Both in vitro and in vivo composite tests showed excellent antibacterial activity against drug-resistant pathogenic bacteria.

Recently, researchers discovered that Ag nanoclusters (NCs) are effective for this type of application [32][33]. NCs are NPs whose sizes are smaller than 2 nm and contain “countable” Ag atoms as a nucleus protected by organic ligands [1]. Ag NCs have shown promising results for biomedical applications, such as bioimaging, biosensing, and antimicrobial agents [34][35]. These NPs have also been used to functionalize natural cellulose nanofibers [36], silk fibers [37], textiles [38], and natural or synthetic polymer-based hydrogels to exhibit antimicrobial activity. Although there are many studies of antimicrobial Ag NPs embedded into hydrogels as platforms for delivering metallic nanostructures as alternative to standard drugs; their mechanism of action has not been entirely elucidated. Nevertheless, all the above examples demonstrate this as a promising strategy in preventing and eradicating infections [39][40].

2. Antibacterial Activity of Ag NPs Loaded into Hydrogels

Ag NPs incorporated into hydrogels have shown antibacterial properties and the ability to control infections [41]. The NPs are incorporated into a hydrogel with a porous structure by in situ polymer synthesis or by adding the NP colloid to the polymer. Additionally, microwave radiation is another approach to produce NPs within hydrogels. The polymer-based hydrogels help to control the morphology and size of the nanostructures and participate as a stabilizing medium for nucleation sites to produce silver seeds [17][19]. Biocompatible polymers, such as chitosan [42], konjac glucomannan [43], carboxymethyl cellulose [17], carboxymethyl chitosan [44], polyvinyl alcohol [41], carbopol-934 [45], graphene [46][47][48][49], gelatin methacrylate [50], polyacrylamide [51], polyethyleneimine [19], and polyvinylpyrrolidone [26][45][51][52][53], have been used to fabricate antibacterial and antibiofilm materials.

These polymeric biomaterials have helped to treat and prevent infections caused by pathogenic bacteria and are capable of improving the healing and regeneration of the skin. For example, Ag/chitosan/hydrogel has been shown to help the healing process, reduced inflammation at skin wounds, and accelerated the re-epithelization rate to treat post-operative infection [18].

Chitosan (CS) is derived from chitin, the second most abundant biopolymer in nature, after cellulose. It has been used in the synthesis of hydrogels due to its biodegradability, biocompatibility, and antibacterial activity [18]. Chemical crosslinking, the addition of nanofillers, blending with other polymers, and using alkali–urea solutions, are some of the methods used to improve chitosan processability. To improve the water solubility of chitosan, quaternization method has been used, in which a quaternary ammonium moiety was introduced into the chitosan structure by chemical reactions, thus producing quaternate chitosan. Some studies have reported the use of chitosan as a matrix to incorporate Ag nanoparticles. Ag NPs were also synthesized in situ within oxidized dextran (ODex), adipic dihydrazide-grafted hyaluronic acid (HA-ADH), and quaternized chitosan (HACC), resulting in the Ag–ODex/HA-ADH/HACC hydrogel [42]. The Ag NPs had a particle distribution size of around 50–190 nm. The hydrogel displayed antibacterial properties against *E. coli* ATCC 8739, *S. aureus* ATCC 14458, and *P. aeruginosa* CMCCB10104, and the inhibition zones were 24, 24, and 27 mm, respectively. These results were associated with the hydrogel’s positive charge due to the quaternate chitosan’s cationic group, that favor the interaction with the negatively charged bacterial cell walls. This system reduced the wound area in rats up to 41.3% after 7 days, decreased inflammation, and improved re-epithelialization [42].

In a similar study, Xie et al. [18] prepared an Ag/chitosan hydrogel using an alkali–urea solution, LiOH (4.5% wt.)/KOH (7% wt.)/CH_4N_2O (8% wt.) by the freeze/thaw process, $AgNO_3$, and $Na_3C_6H_5O_7$. The silver concentration in the hydrogel increased, leading to spherical and ellipsoidal Ag NPs with a size distribution of 4.45 nm ± 0.37 nm to 9.22 ± 0.54 nm. The hydrogel composite had large tensile mechanical properties (15.95 ± 1.95 MPa). The antimicrobial activity was 99.86 ± 0.12% against *E. coli* and 99.94 ± 0.10% against *S. aureus* tested on rats for 14 days. The wound contraction was 70.5% on the 4th day and 99.75% on the 14th day. Thus, Ag NPs coated with chitosan accelerated the healing process. The authors determined that Ag NPs destroyed the bacterial cell wall due to interactions between the NPs and the lipid layer of the bacterial cell membrane. The Ag NPs would merge with bacterial DNA damaging bacterial replication and impairing bacterial respiratory function.

Furthermore, carboxymethyl chitosan is a derivative of chitosan, non-toxic, and also capable of forming gels [44]. Carboxymethyl chitosan-based hydrogels have shown enhanced physicochemical, and biological properties, including antimicrobial, antioxidant, and antifungal activities. This hydrogel has been used in applications such as wound healing,

drug-carrying, smart tissue, and biomedical nanodevices [54]. Additionally, it has been well explored in the cosmetic and food industry [44].

Ag/chitosan-carboxymethyl β-cyclodextrin hydrogel (CM-βCD) is an alternative approach to inhibit the growth of bacteria. It has been shown to display antibacterial activity against *E. coli* and *S. aureus* [55]. The interactions between Ag^+ ions and bacteria were improved through ions exchange between Ag^+ and H^+ from the carboxylic and amino groups within the Ag NPs-CM-βCD hydrogel. The inhibition zone increased when the concentration of CM-βCD was increased in the hydrogel [55].

Pandian et al. [41] fabricated a Ag/N, O-carboxymehtyl chitosan (N, O-CMC) hydrogel with self-healing properties. The ethylenediaminetetraacetic acid (EDTA, $C_{10}H_{16}N_2O_8$) and ferric ions (Fe^{3+}, $FeCl_3$, 2%) were used in the synthesis process to produce a self-healing hydrogel. The size distribution of Ag NPs was 25 ± 14 nm according to TEM images. The hydrogel displayed an antibacterial activity against ATCC and clinical strains of *E. coli* ATCC 25922, *S. aureus* ATCC 35556, MRSA ATCC 43300, *P. aeruginosa* ATCC 47085, and *K. pneumonia* ATCC 700603. The minimum inhibitory concentration (MIC) for *P. aeruginosa* was 48.5 mg/mL, 32.5 mg/mL for MRSA, and 32 mg/mL for *S. aureus*. The Ag NPs/N, O-CMC hydrogel was more efficient against *E. coli* and *K. pneumonia* with MIC values of 17.5 and 23.0 mg/mL, respectively. At the same time, the minimum bactericidal concentration (MBC) values were 55 and 71 mg/mL, respectively. The authors described that the interaction between Fe^{3+} (metal) and -COOH (ligand) was responsible for the self-healing property of the Ag NPs/N, O-CMC hydrogel [41].

The carboxymethyl chitosan (CMCS) has been mixed with oxidized konjac glucomannan (OKGM). The OKGM is a natural polysaccharide, soluble in water, that was shown to improve the microstructure and mechanical properties of chitosan [56] [57], gelatin [58], and oxidized hyaluronic acid [59], acting as a macromolecular cross-linker [57]. The OKGM-based hydrogel exhibited self-healing characteristics in a recent study, where Ag NPs/OKGM/CMCS hydrogel demonstrated antibacterial properties against *E. coli* and *S. aureus* [43]. This hydrogel was tested on rats' skin. The hydrogel pore size distribution was in the range of 59.4 to 230 µm, increasing as the concentration of OKGM increased, but the swelling capacity decreased. Higher concentrations of polymers accelerated the gelation time from 600 to 57 s [43]. Similar to a previous study, Ag/konjac glucomannan hydrogel was tested against *S. aureus* and *E. coli* showing good antibacterial efficiency on rabbit skin infections [60].

Hydrogels based on carboxymethyl cellulose (CMC), polyvinyl alcohol (PVA), and $C_8H_{14}O_4$ (EDGE) has been prepared using microwave radiation as a carrier of Ag NPs (8–14 nm). The Ag release rate from this hydrogel was 85% over five days [17]. Ag^+ ions are bound to the hydrogel composite via electrostatic interactions. This Ag/hydrogel acted as a bactericide against pathogenic microorganisms of the urinary tract, such as *E. coli*, *K. pneumoniae*, *P. aeruginosa*, *P. vulgaris*, *S. aureus*, and *P. mirabilis* [17]. The Ag/hydrogels with 5 mg/mL of Ag presented a growth inhibition diameter of 16.6 mm against *E. coli*, 15.8 mm against *K. pneumoniae*, 15.6 mm against *P. aeruginosa*, and 15.2 mm against *P. vulgaris*.

Hydrogels based on carbopol-934 and *Aloe vera* supported Ag spherical NPs encapsulating quercetin (QCT) [45]. This system was designed to take advantage of (i) the properties of QCT as an anti-inflammatory and antioxidant; (ii) of carbopol-934, as a biodegradable and bioadhesive polymer with good tensile strength; (iii) *Aloe vera* that stimulates collagen production; and finally, (iv) of Ag NPs that have broad antimicrobial activity. The QCT-Ag/carbopol-*Aloe vera* hydrogel presented antibacterial activity against *S. aureus* MTCC 3160 and *E. coli* BL-21 with inhibition zone values of about 19.0 and 17.0 mm, respectively. Ag NPs improved the release rate of quercetin from the hydrogel for the treatment of wounds in diabetic patients.

Some studies have explored the incorporation of graphene into hydrogel structures due to its high thermal and electrical conductivity, and sizeable mechanical strength [19][47][48][49]. The graphene embedded in hydrogel reduced hydrogel breaking and reinforced its mechanical properties. The Ag/graphene composite hydrogel was prepared using acrylic acid and N,N′-methylene bisacrylamide ($C_7H_{10}N_2O_2$), with a mass ratio of 5:1 silver to graphene [46]. The Ag NPs of an average size of 39 nm were deposited onto the surface of graphene nanosheets. The Ag NPs/graphene hydrogel was evaluated against *E. coli* and *S. aureus* using the shaking flask method. The antimicrobial activity was enhanced as the Ag NP concentration increased. Larger nanoparticle sizes displayed better antimicrobial activity than smaller ones. The graphene promoted the incorporation of a higher number of NPs and avoided their aggregation onto its surface.

Another approach that has been explored is to combine chitosan and graphene to produce an antibacterial hydrogel with enhanced durability [48]. For instance, Nešović et al. prepared Ag/poly(vinyl alcohol)/chitosan/graphene hydrogels [47][48][49] by electrochemical synthesis of nanoparticles in a hydrogel network. The hydrogel displayed better mechanical characteristics, such as tensile strength and elastic modulus. The Ag NPs size distribution was from 6.38 to 10.00 nm depending on the chitosan content. The antimicrobial activity was evaluated against *E. coli* ATCC 25922 and *S. aureus* TL. The number of bacteria colonies decreased quickly in 15 min, when the $AgNO_3$ concentration was 0.25 mM and 0.5% wt. of chitosan, during the composite hydrogel preparation (0.25Ag/PVA/0.5CHI/Gr). Increasing the chitosan content

resulted in a slower Ag release rate from the hydrogel. Nešović et al. [48] found that Ag NPs prevented adenosine 5′-triphosphate (ATP) formation within the microorganism.

Figure 1 summarizes the hydrogels embedded with Ag and gold (Au) NPs against multidrug-resistant bacteria.

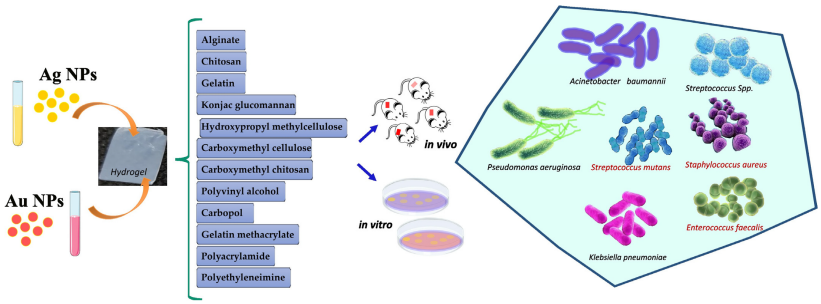

Figure 1. Silver and gold NPs loaded into hydrogels for antibacterial application.

A Ag-polyethyleneimine (PEI)-graphene oxide (GO) hydrogel was produced using Pluronic F127 gel [19]. In this case, Pluronic F-127 was used to create a sustained antimicrobial effect, presenting reverse thermal gelation properties. PEI decreased the aggregation of nanostructures within the hydrogel. The antimicrobial activity against *E. coli* was 99.86%, and 99.94% against *C. albicans*, using 10 µg/mL of the hydrogel. The Ag release rate from the hydrogel was 72% in 7 days. The authors proposed that the graphene oxide nanosheets damaged the bacterial cell wall due to the sharp edges leading to a faster disruption of the plasmatic membrane by the Ag NPs.

Furthermore, Ag NPs have been incorporated into nanotubes/polymer hydrogels to explore NP delivery. For instance, aluminosilicate nanotubes (NTs) are platforms with a great capacity to store and carry molecules and drugs. They also help to reduce the hydrogel degradation rate and can be loaded, as additives, into the hydrogels, such as gelatin methacrylate (GelMA), a biocompatible hydrogel with many biological characteristics [61]. For example, Ag NPs were loaded into aluminosilicate nanotubes (NTs) and then within a methacrylate gelatin [50] matrix, to produce an antibacterial hydrogel capable of improving bone regeneration. The hydrogel was prepared using photopolymerization by UV irradiation of 365 nm and 400 W. According to the inhibition zone results, the Ag/NTs/GelMA hydrogel showed higher antibacterial activity against *E. coli* ATCC 8739 than *S. aureus* ATCC 29213.

In addition, the morphology of Ag NPs is another relevant aspect that influences a hydrogel's antibacterial efficiency. Different NP shapes may present a distinct surface area to interact with bacterial membranes, leading to diverse antibacterial activity [51][62][63]. In this context, Ag NPs with different morphologies (spherical, triangular, and rod) were incorporated into polyacrylamide (PPA) and N-mehtylene bisacrylamide (MBA) hydrogels, named PAA-MBA [51]. The mechanical strength of the Ag NPs-PAA-MBA hydrogel (4 to 5 KPa) did not depend on Ag NP shape. Rod-shaped nanoparticles were poorly absorbed within the hydrogel network due to the formation of aggregates on the hydrogel surface. However, these NPs showed antibacterial activity. The hydrogel doped with spherical NPs of 12.7 ± 5.9 nm and triangular NPs of 37.1 ± 15.0 nm demonstrated high antimicrobial activity against *E. coli.*

Table 1 summarizes the hydrogels embedded with Ag NPs for antibacterial application.

Table 1. Ag NPs loaded into hydrogel for antibacterial application.

System	Materials	Ag NP Properties (Size and Surface Charge)	NP Synthesis Method	Bacteria	Target	Antibacterial Properties: Inhibition Zone (mm) and MIC Values
Ag–ODex HA-ADH/HACC	Dextran, sodium hyaluronic, chitosan quaternary ammonium salt, and $AgNO_3$	50–190 nm	Chemical reduction, in situ, Schiff-base reaction to form hydrogel	*E. coli* ATCC8739, *S. aureus* ATCC14458, and *P. aeruginosa* CMCCB10104	In vitro; In vivo, rats	The Kirby–Bauer (KB) method. The inhibition zone was 24, 24, and 27 mm, respectively
Ag/CS	LiOH, KOH, CH_4N_2O, $AgNO_3$, and $Na_3C_6H_5O_7$	Spherical and ellipsoidal NPs; 4.45–9.22 nm	Chemical reduction with sodium citrate, in situ	*E. coli* and *S. aureus*	In vivo; rats	Antibacterial activity: 99.86% and 99.94%, respectively
Ag/CM- βCD	Chitosan, $NaBH_4$, $AgNO_3$, NaOH, cyclodextrin, CH_3CO_2H, and C_5H_8O	50 nm	Chemical reduction with $NaBH_4$, in situ	*E. coli* and *S. aureus*	In vitro	The inhibition zone increased when the CM-βCD concentration was increased in the hydrogel

System	Materials	Ag NP Properties (Size and Surface Charge)	NP Synthesis Method	Bacteria	Target	Antibacterial Properties: Inhibition Zone (mm) and MIC Values
Ag/N, O-carboxymehtyl chitosan (N, O-CMC)	Chitosan, $AgNO_3$, $C_{10}H_{16}N_2O_8$ (EDTA), $CaCl_2$, $FeCl_3$, and $C_2H_3ClO_2$	25 nm	Chemical reduction using $C_2H_3ClO_2$	*E. coli* ATCC25922, *S. aureus* ATCC35556, MRSA ATCC 43300, *P. aeruginosa* ATCC47085, and *K. pneumonia* ATCC700603	In vitro, L929 cells	MIC values: 48.5 mg/mL for *P. aeruginosa;* 32.0 mg/mL for *S. aureus* and MRSA; 17.5 mg/mL for *E. coli*, and 23.0 mg/mL for *K. pneumonia*
Ag/OKGM-CMCS	Oxidized konjac glucomannan (OKGM) and Carboxymethyl chitosan (CMCS)	60 nm	Schiff-base reaction	*S. aureus* and *E. coli*	In vitro, L929 cells; In vivo, rats	The Ag/hydrogel achieved high antimicrobial activity, but the inhibition zone values were not displayed
Ag/KGM	Eggs, konjac glucomannan, $AgNO_3$, and NaOH	9.5–30.2 nm	In situ	*S. aureus* and *E. coli*	In vitro; In L929 cells; in vivo, rabbits	Good antibacterial efficiency on rabbits' skin infections
Ag/CMC/PVA/EGDE	Carboxymethyl cellulose (CMC), polyvinyl alcohol (PVA), and ethylene glycol diglycidyl ether (EGDE)	8–14 nm	Microwave radiation	*E. coli*, *K. pneumoniae*, *P. aeruginosa*, *Proteus vulgaris*, *S. aureus*, and *Proteus mirabilis*	In vitro, patient urine	The inhibition zone: 16.6 mm for *E. coli*, 15.8 mm for *K. pneumoniae*, 15.6 mm for *P. aeruginosa* and 15.2 mm for *P. vulgaris*
QCT-Ag/Carbopol- *aloe vera*	Carbopol 934, $AgNO_3$, QCT, polyvinylpyrrolidone (PVP), *Aloe vera*, $C_3H_8O_3$, and $NaBH_4$	44.1 nm; ζ: −14.76 mV	Chemical reduction with $NaBH_4$	*S. aureus* MTCC 3160 and *E. coli* BL-21	In vitro, L929 cells; In vivo, mice skin	The inhibition zone: 17 mm for *E. coli* and 19 mm for *S. aureus*
Ag/graphene	$AgNO_3$, $C_7H_{10}N_2O_2$, $(NH_4)_2S_2O_8$, and NH_3H_2O	39 nm	Hummer's method	*E. coli* and *S. aureus*	In vitro, L929 cells; In vivo, rats	The disc diffusion method. Large Ag concentration led to great antibacterial activity using 5:1% wt. of Graphene
Ag/poly(vinyl alcohol)/chitosan/graphene	Graphene, chitosan, CH_3CO_2H, KNO_3, $AgNO_3$, and K_2HPO_4	6.38–10.00 nm	Electrochemical synthesis in situ using 90 V	*E. coli* ATCC 25922 and *S. aureus* TL	In vitro, MRC-5 and L929 cells;	The inhibition zone: 15.5 mm for *S. aureus* and 13.5 mm for *E. coli*; great antimicrobial activity with the 0.25Ag/PVA/0.5CHI/Gr
Ag/PEI- graphene oxide	Pluronic F 127, graphene oxide, $C_8H_{17}N_3$.HCl, $AgNO_3$, NH_4OH, and NaCl	10 nm; ζ: 42.6 mV	Amidation reaction with $Ag(NH_3)_2OH$ by microwave reactor	*E. coli* and *C. albicans*	In vitro	*E. coli* (99.86%) and *C. albicans* (99.94%)
Ag/PAA-MBA	$K_2S_2O_8$, $NaBH_4$, PVP, C_3H_5NO, $C_6H_9Na_3O_9$, and $AgNO_3$	Spherical: 12.7 nm; triangular: 37.1 nm; hexagonal: 26.9 nm	Chemical reduction using $NaBH_4$	*E. coli* W3110	In vitro	The spherical and triangular shapes of the Ag NPs displayed better antibacterial activity than the rod-shaped NPs.

System	Materials	Ag NP Properties (Size and Surface Charge)	NP Synthesis Method	Bacteria	Target	Antibacterial Properties: Inhibition Zone (mm) and MIC Values
Ag/halloysite/gelatin methacrylate	$AgNO_3$, $NaBH_4$, $(CH_3)_2SO$, and C_2H_4O	Ag NPs changed the microstructure and roughness of the hydrogel	In situ by photopolymerization using UV radiation (365 nm and 400 W)	*E. coli* ATCC 8739 and *S. aureus* ATCC 29213	In vitro; In vivo, crania of rats	The inhibition zone test showed that the hydrogel restrained the growth of the bacteria
Ag/KGM	Chitosan, carboxymethyl, β-cyclodextrin, etc.	50 nm	Chemical reduction	*S. aureus* and *E. coli*	In vitro	Inhibition zone: 22 and 19 mm, respectively

3. Antibiofilm Activity of Hydrogels Loaded with Ag NPs

Taking the usefulness of non-invasive therapy into consideration, and the elimination of drug-resistant biofilms in oral infections and wound healing, hydrogels loaded with Ag NPs is an alternative method of infection management [64][65][66]. In this scenario, Haidari et al. [67] investigated the effectiveness of applied Ag NP hydrogels in mature *S. aureus* biofilms, both in vitro and in vivo. In vitro tests were performed by flow cytometry, where bacterial cells with compromised membranes were stained red by propidium iodide, whereas cells with intact membranes were stained green by SYTO9. The test showed that after treating the *S. aureus* biofilm with the Ag NP hydrogel, most of the cells were stained in a high red fluorescence intensity, associated with a substantially lower biofilm biomass, indicating severe disruption of the mature biofilm. For in vivo tests, an established *S. aureus* mouse model of a mature biofilm wound infection was utilized. The antibiofilm treatment started after biofilms had been fully established. IVIS bioluminescent imaging was used to track 10 days of Ag NP hydrogel treatment in real-time. The Ag NP hydrogel treatment gradually decreased the *S. aureus* biofilm starting on day 4. From 5 to 10 days after the infection, there was a statistically significant decrease in the concentration of bacterial cells, showing the high efficiency of the Ag NPs in eradicating established mature biofilms in wounds. This study demonstrated the use of an Ag NP hydrogel as a valid therapeutic approach for the effective and safe elimination of mature *S. aureus* biofilms in wounds.

Consistent with these results, Imran et al. [68], also reported the antibiofilm activity of a Ag NP-loaded hydrogel against *B. subtilis* and *E. coli*. It was revealed that the hydrogel showed a dose-dependent biofilm inhibition activity, with a minimum biofilm inhibition of approximately 27% when the Ag NPs were used at a concentration of 10 ppm and a maximum inhibition of 97% when the Ag NPs were used at a concentrations of 100 ppm. Additionally, the half maximal inhibitory concentration (IC_{50}) values obtained were 29.88 and 27.36 for *E. coli* and *B. subtilis*, respectively. Pandian et al. [41], in turn, evaluated the antibiofilm activity of in situ Ag NPs incorporated in an N, O-carboxymethyl chitosan self-healing hydrogel. After 48 h, a decrease of 68.86 ± 0.05%, 75.07 ± 0.02%, and 83.22 ± 0.01% was observed in *E. coli*-, *S. aureus*-, and *P. aeruginosa*-treated biofilms, respectively.

Alfuraydi et al. [69] described the preparation of novel cross-linked chitosan and PVA hydrogels impregnated with Ag NPs, as well as its activity against different strains of fungi, Gram-positive and Gram-negative bacteria. In their results, The minimal biofilm inhibition concentration (MBIC) for the chitosan hydrogels alone ranged from 15.63 to 125 µg/mL, differing from the MBIC values of the hydrogel containing Ag NPs at 1 and 3%, which ranged from 1.95 to 7.81 µg/mL. These data demonstrated how the dispersion of Ag NPs inside the matrix of the chitosan hydrogel significantly improved its ability to prevent the formation of biofilms.

Similarly, the antibiofilm action of the chitosan hydrogel containing Ag NPs was previously explored by Pérez-Díaz et al. [70]. In their work, the hydrogels demonstrated a great impact on the multi-species biofilm of oxacillin-resistant *S. aureus* (ORSA), achieving a 6 Log_{10} reduction at a Ag NP concentration of 100 ppm. The antibiofilm activity against *P. aeruginosa* was lower, with a Log_{10} decrease of 3.3 at a concentration of 1000 ppm. As stated in the study conducted by Arinah et al. [71], the different results on the tested drugs' antibiofilm activity could be attributed to structural variations in the bacterial membrane walls, which differ in Gram-negative or Gram-positive bacteria. In their work, the authors incorporated *Pleurotus ostreatus*-biosynthesized Ag NPs into a genipin-crosslinked gelatin hydrogel to investigate the antibiofilm properties against the biofilms of *S. aureus*, *P. aeruginosa*, *Bacillus* sp., and *E. coli*. Stronger biofilm inhibition of about 58 ± 4% was observed in Gram-negative strains. For Gram-positive bacteria, the percentage of inhibition was 55 ± 5% for *S. aureus* and 38 ± 1% for *Bacillus* spp.

Furthermore, many recent studies have reported antibacterial and antibiofilm activity improvement of drugs when they are associated with metallic nanoparticles, such as Ag NPs [72][73]. Thus, in the research conducted by Lopez-Carrizales et al. [74], chitosan hydrogel loaded with Ag NPs and the antibiotic ampicillin (AMP) were tested against resistant bacterial pathogens, evaluating its capacity to prevent the early formation of biofilms by the colony biofilm model. The biofilm produces thick, layered structures, and the counting of colony-forming units (CFU) was Log_{10}-transformed. The antibiofilm action of the hydrogel changed depending on the Ag NP and ampicillin concentrations and the tested strain. The biofilms

of *A. baumannii*, *E. faecium*, and *S. epidermidis*, were significantly inhibited by the hydrogel with the lowest concentration of Ag NPs and ampicillin (25 ppm Ag NPs/50 ppm AMP), exhibiting Log_{10} reductions of 10 ± 0.01, 8.9 ± 0.02, and 7.8 ± 0.13, respectively. However, the *E. cloacae* biofilm was only inhibited by a higher antimicrobial dose (250 ppm Ag NPs/500 ppm AMP), resulting in a Log_{10} reduction of 9.9 ± 0.11.

Recently, Wunno et al. [75] investigated a potentially new sustainable delivery system of Ag NPs for, among other activities, antibiofilm action. In their work, an ex situ thermosensitive hydrogel based on poloxamers loaded with biosynthesized Ag NPs from *Eucalyptus camaldulensis* was created and tested against Gram-positive (*S. aureus* and *S. epidermidis*) and Gram-negative bacterial (*A. baumannii* and *P. aeruginosa*) biofilms. At a ½ minimum inhibitory concentration (MIC), the proportion of biofilm inhibition reached 83%. When the mature biofilms were exposed to the Ag NP hydrogel and analyzed by confocal laser scanning, loosening of the biofilm architecture and cell death were revealed after 4 h of co-incubation with the hydrogel formulation at a 2 MIC (µg/mL) concentration. Based on the presented results, it is clear that the tested hydrogel formulation successfully interrupted biofilm formation and eradicated cell viability within the mature biofilms.

References

1. Zheng, K.; Setyawati, M.I.; Leong, D.T.; Xie, J. Antimicrobial silver nanomaterials. Coord. Chem. Rev. 2018, 357, 1–17.
2. Kujda, M.; Wieja, M.; Adamczyk, Z.; BocheSka, O.; Bra, G.; Kozik, A.; BielaSka, E.; Barbasz, J. Charge Stabilized Silve r Nanoparticles Applied as Antibacterial Agents. J. Nanosci. Nanotechnol. 2015, 15, 3574–3583.
3. Alavi, M.; Karimi, N. Biosynthesis of Ag and Cu NPs by secondary metabolites of usnic acid and thymol with biological macromolecules aggregation and antibacterial activities against multi drug resistant (MDR) bacteria. Int. J. Biol. Macro mol. 2019, 128, 893–901.
4. Aurore, V.; Caldana, F.; Blanchard, M.; Kharoubi Hess, S.; Lannes, N.; Mantel, P.-Y.; Filgueira, L.; Walch, M. Silver-nan oparticles increase bactericidal activity and radical oxygen responses against bacterial pathogens in human osteoclast s. Nanomed. Nanotechnol. Biol. Med. 2018, 14, 601–607.
5. Beyene, H.D.; Werkneh, A.A.; Bezabh, H.K.; Ambaye, T.G. Synthesis paradigm and applications of silver nanoparticles (AgNPs), a review. Sustain. Mater. Technol. 2017, 13, 18–23.
6. Feizi, S.; Taghipour, E.; Ghadam, P.; Mohammadi, P. Antifungal, antibacterial, antibiofilm and colorimetric sensing of tox ic metals activities of eco friendly, economical synthesized Ag/AgCl nanoparticles using Malva Sylvestris leaf extracts. Microb. Pathog. 2018, 125, 33–42.
7. Lok, C.-N.; Ho, C.-M.; Chen, R.; He, Q.-Y.; Yu, W.-Y.; Sun, H.; Tam, P.K.-H.; Chiu, J.-F.; Che, C.-M. Silver nanoparticles: Partial oxidation and antibacterial activities. JBIC J. Biol. Inorg. Chem. 2007, 12, 527–534.
8. Yusuf, M. Handbook of Ecomaterials; Martínez, L.M.T., Kharissova, O.V., Kharisov, B.I., Eds.; Springer International Pu blishing: Cham, Switzerland, 2019; pp. 2343–2356.
9. Sondi, I.; Salopek-Sondi, B. Silver nanoparticles as antimicrobial agent: A case study on E. coli as a model for Gram-ne gative bacteria. J. Colloid Interface Sci. 2004, 275, 177–182.
10. Morones, J.R.; Elechiguerra, J.L.; Camacho, A.; Holt, K.; Kouri, J.B.; Ramírez, J.T.; Yacaman, M.J. The bactericidal effe ct of silver nanoparticles. Nanotechnology 2005, 16, 2346–2353.
11. Ansari, M.A.; Khan, H.M.; Khan, A.A.; Ahmad, M.K.; Mahdi, A.A.; Pal, R.; Cameotra, S.S. Interaction of silver nanoparti cles with Escherichia coli and their cell envelope biomolecules. J. Basic Microbiol. 2014, 54, 905–915.
12. Mirzajani, F.; Ghassempour, A.; Aliahmadi, A.; Esmaeili, M.A. Antibacterial effect of silver nanoparticles on Staphylococ cus aureus. Res. Microbiol. 2011, 162, 542–549.
13. Kim, J.S.; Kuk, E.; Yu, K.N.; Kim, J.-H.; Park, S.J.; Lee, H.J.; Kim, S.H.; Park, Y.K.; Park, Y.H.; Hwang, C.-Y.; et al. Anti microbial effects of silver nanoparticles. Nanomed. Nanotechnol. Biol. Med. 2007, 3, 95–101.
14. Hwang, E.T.; Lee, J.H.; Chae, Y.J.; Kim, Y.S.; Kim, B.C.; Sang, B.-I.; Gu, M.B. Analysis of the Toxic Mode of Action of Si lver Nanoparticles Using Stress-Specific Bioluminescent Bacteria. Small 2008, 4, 746–750.
15. Sies, H. Oxidative stress: Oxidants and antioxidants. Exp. Physiol. 1997, 82, 291–295.
16. Dibrov, P.; Dzioba, J.; Gosink, K.K.; Häse, C.C. Chemiosmotic Mechanism of Antimicrobial Activity of Ag+ in Vibrio chol erae. Antimicrob. Agents Chemother. 2002, 46, 2668–2670.
17. Alshehri, S.M.; Aldalbahi, A.; Al-Hajji, A.B.; Chaudhary, A.A.; Panhuis, M.I.H.; Alhokbany, N.; Ahamad, T. Development o f carboxymethyl cellulose-based hydrogel and nanosilver composite as antimicrobial agents for UTI pathogens. Carboh ydr. Polym. 2016, 138, 229–236.
18. Xie, Y.; Liao, X.; Zhang, J.; Yang, F.; Fan, Z. Novel chitosan hydrogels reinforced by silver nanoparticles with ultrahigh mechanical and high antibacterial properties for accelerating wound healing. Int. J. Biol. Macromol. 2018, 119, 402–41 2.

19. Yang, S.; Zhou, Y.; Zhao, Y.; Wang, D.; Luan, Y. Microwave synthesis of graphene oxide decorated with silver nanoparti cles for slow-release antibacterial hydrogel. Mater. Today Commun. 2022, 31, 103663.

20. Gnanadhas, D.P.; Ben Thomas, M.; Thomas, R.; Raichur, A.M.; Chakravortty, D. Interaction of Silver Nanoparticles with Serum Proteins Affects Their Antimicrobial Activity In Vivo. Antimicrob. Agents Chemother. 2013, 57, 4945–4955.

21. Agnihotri, S.; Mukherji, S.; Mukherji, S. Size-controlled silver nanoparticles synthesized over the range 5–100 nm using the same protocol and their antibacterial efficacy. RSC Adv. 2014, 4, 3974–3983.

22. Feng, Y.; Min, L.; Zhang, W.; Liu, J.; Hou, Z.; Chu, M.; Li, L.; Shen, W.; Zhao, Y.; Zhang, H. Zinc Oxide Nanoparticles Inf luence Microflora in Ileal Digesta and Correlate Well with Blood Metabolites. Front. Microbiol. 2017, 8, 992.

23. Sadeghi, B.; Garmaroudi, F.S.; Hashemi, M.; Nezhad, H.R.; Nasrollahi, A.; Ardalan, S.; Ardalan, S. Comparison of the a nti-bacterial activity on the nanosilver shapes: Nanoparticles, nanorods and nanoplates. Adv. Powder Technol. 2012, 2 3, 22–26.

24. Zhang, Y.; Peng, H.; Huang, W.; Zhou, Y.; Yan, D. Facile preparation and characterization of highly antimicrobial colloid Ag or Au nanoparticles. J. Colloid Interface Sci. 2008, 325, 371–376.

25. Ivask, A.; ElBadawy, A.; Kaweeteerawat, C.; Boren, D.; Fischer, H.; Ji, Z.; Chang, C.H.; Liu, R.; Tolaymat, T.; Telesca, D.; et al. Toxicity Mechanisms in Escherichia coli Vary for Silver Nanoparticles and Differ from Ionic Silver. ACS Nano 2 014, 8, 374–386.

26. Tejamaya, M.; Römer, I.; Merrifield, R.C.; Lead, J.R. Stability of Citrate, PVP, and PEG Coated Silver Nanoparticles in E cotoxicology Media. Environ. Sci. Technol. 2012, 46, 7011–7017.

27. Abbaszadegan, A.; Ghahramani, Y.; Gholami, A.; Hemmateenejad, B.; Dorostkar, S.; Nabavizadeh, M.; Sharghi, H. The effect of charge at the surface of silver nanoparticles on antimicrobial activity against gram-positive and gram-negative bacteria: A preliminary study. J. Nanomater. 2015, 16, 53.

28. Fayaz, A.M.; Balaji, K.; Girilal, M.; Yadav, R.; Kalaichelvan, P.T.; Venketesan, R. Biogenic synthesis of silver nanoparticl es and their synergistic effect with antibiotics: A study against gram-positive and gram-negative bacteria. Nanomed. Na notechnol. Biol. Med. 2010, 6, 103–109.

29. Banerjee, M.; Mallick, S.; Paul, A.; Chattopadhyay, A.; Ghosh, S.S. Heightened Reactive Oxygen Species Generation i n the Antimicrobial Activity of a Three Component Iodinated Chitosan−Silver Nanoparticle Composite. Langmuir 2010, 26, 5901–5908.

30. Mishra, S.K.; Raveendran, S.; Ferreira, J.M.F.; Kannan, S. In Situ Impregnation of Silver Nanoclusters in Microporous Chitosan-PEG Membranes as an Antibacterial and Drug Delivery Percutaneous Device. Langmuir 2016, 32, 10305–10 316.

31. Liang, D.; Lu, Z.; Yang, H.; Gao, J.; Chen, R. Novel Asymmetric Wettable AgNPs/Chitosan Wound Dressing: In Vitro an d In Vivo Evaluation. ACS Appl. Mater. Interfaces 2016, 8, 3958–3968.

32. Jin, R.; Zeng, C.; Zhou, M.; Chen, Y. Atomically Precise Colloidal Metal Nanoclusters and Nanoparticles: Fundamentals and Opportunities. Chem. Rev. 2016, 116, 10346–10413.

33. Fang, J.; Zhang, B.; Yao, Q.; Yang, Y.; Xie, J.; Yan, N. Recent advances in the synthesis and catalytic applications of lig and-protected, atomically precise metal nanoclusters. Coord. Chem. Rev. 2016, 322, 1–29.

34. Tao, Y.; Li, M.; Ren, J.; Qu, X. Metal nanoclusters: Novel probes for diagnostic and therapeutic applications. Chem. So c. Rev. 2015, 44, 8636–8663.

35. Luo, Z.; Zheng, K.; Xie, J. Engineering ultrasmall water-soluble gold and silver nanoclusters for biomedical applications. Chem. Commun. 2014, 50, 5143–5155.

36. Díez, I.; Eronen, P.; Österberg, M.; Linder, M.B.; Ikkala, O.; Ras, R.H.A. Functionalization of Nanofibrillated Cellulose wi th Silver Nanoclusters: Fluorescence and Antibacterial Activity. Macromol. Biosci. 2011, 11, 1185–1191.

37. Wang, X.; Gao, W.; Xu, S.; Xu, W. Luminescent fibers: In situ synthesis of silver nanoclusters on silk via ultraviolet light-induced reduction and their antibacterial activity. Chem. Eng. J. 2012, 210, 585–589.

38. Balagna, C.; Irfan, M.; Perero, S.; Miola, M.; Maina, G.; Santella, D.; Simone, A. Characterization of antibacterial silver nanocluster/silica composite coating on high performance Kevlar® textile. Surf. Coat. Technol. 2017, 321, 438–447.

39. Panáček, A.; Kvítek, L.; Smékalová, M.; Večeřová, R.; Kolář, M.; Röderová, M.; Dyčka, F.; Šebela, M.; Prucek, R.; Tom anec, O.; et al. Bacterial resistance to silver nanoparticles and how to overcome it. Nat. Nanotechnol. 2018, 13, 65–71.

40. Willing, B.P.; Pepin, D.M.; Marcolla, C.S.; Forgie, A.J.; Diether, N.E.; Bourrie, B.C.T. Bacterial resistance to antibiotic alt ernatives: A wolf in sheep's clothing? Anim. Front. 2018, 8, 39–47.

41. Pandian, M.; Selvaprithviraj, V.; Pradeep, A.; Rangasamy, J. In-situ silver nanoparticles incorporated N, O-carboxymeth yl chitosan based adhesive, self-healing, conductive, antibacterial and antibiofilm hydrogel. Int. J. Biol. Macromol. 202 1, 188, 501–511.

42. Chen, X.S.; Zhang, H.M.; Yang, X.; Zhang, W.H.; Jiang, M.; Wen, T.; Wang, J.; Guo, R.; Liu, H.J. Preparation and Appli cation of Quaternized Chitosan- and AgNPs-Base Synergistic Antibacterial Hydrogel for Burn Wound Healing. Molecule s 2021, 26, 4037.

43. Jiang, Y.G.; Huang, J.J.; Wu, X.W.; Ren, Y.H.; Li, Z.A.; Ren, J.A. Controlled release of silver ions from AgNPs using a h ydrogel based on konjac glucomannan and chitosan for infected wounds. Int. J. Biol. Macromol. 2020, 149, 148–157.

44. Shariatinia, Z. Carboxymethyl chitosan: Properties and biomedical applications. Int. J. Biol. Macromol. 2018, 120, 1406 –1419.

45. Badhwar, R.; Mangla, B.; Neupane, Y.R.; Khanna, K.; Popli, H. Quercetin loaded silver nanoparticles in hydrogel matric es for diabetic wound healing. Nanotechnology 2021, 32, 505102.

46. Fan, Z.; Liu, B.; Wang, J.; Zhang, S.; Lin, Q.; Gong, P.; Ma, L.; Yang, S. A Novel Wound Dressing Based on Ag/Graphe ne Polymer Hydrogel: Effectively Kill Bacteria and Accelerate Wound Healing. Adv. Funct. Mater. 2014, 24, 3933–3943.

47. Nešović, K.; Mišković-Stanković, V. Silver/poly(vinyl alcohol)/graphene hydrogels for wound dressing applications: Und erstanding the mechanism of silver, antibacterial agent release. J. Vinyl Addit. Technol. 2022, 28, 196–210.

48. Nešović, K.; Janković, A.; Perić-Grujić, A.; Vukašinović-Sekulić, M.; Radetić, T.; Živković, L.; Park, S.-J.; Yop Rhee, K.; Mišković-Stanković, V. Kinetic models of swelling and thermal stability of silver/poly(vinyl alcohol)/chitosan/graphene hy drogels. J. Ind. Eng. Chem. 2019, 77, 83–96.

49. Nesovic, K.; Jankovic, A.; Kojic, V.; Vukasinovic-Sekulic, M.; Peric-Grujic, A.; Rhee, K.Y.; Miskovic-Stankovic, V. Silver/p oly(vinyl alcohol)/chitosan/graphene hydrogels—Synthesis, biological and physicochemical properties and silver releas e kinetics. Compos. Part B-Eng. 2018, 154, 175–185.

50. Ou, Q.; Huang, K.; Fu, C.; Huang, C.; Fang, Y.; Gu, Z.; Wu, J.; Wang, Y. Nanosilver-incorporated halloysite nanotubes/ gelatin methacrylate hybrid hydrogel with osteoimmunomodulatory and antibacterial activity for bone regeneration. Che m. Eng. J. 2020, 382, 123019.

51. Ferrag, C.; Li, S.P.; Jeon, K.; Andoy, N.M.; Sullan, R.M.A.; Mikhaylichenko, S.; Kerman, K. Polyacrylamide hydrogels d oped with different shapes of silver nanoparticles: Antibacterial and mechanical properties. Colloids Surf. B-Biointerface s 2021, 197, 111397.

52. Ge, J.; Li, Y.; Wang, M.; Gao, C.; Yang, S.; Lei, B. Engineering conductive antioxidative antibacterial nanocomposite hy drogel scaffolds with oriented channels promotes structure-functional skeletal muscle regeneration. Chem. Eng. J. 202 1, 425, 130333.

53. Deng, Z.; Li, M.; Hu, Y.; He, Y.; Tao, B.; Yuan, Z.; Wang, R.; Chen, M.; Luo, Z.; Cai, K. Injectable biomimetic hydrogels e ncapsulating Gold/metal–organic frameworks nanocomposites for enhanced antibacterial and wound healing activity u nder visible light actuation. Chem. Eng. J. 2021, 420, 129668.

54. Fonseca-Santos, B.; Chorilli, M. An overview of carboxymethyl derivatives of chitosan: Their use as biomaterials and dr ug delivery systems. Mater. Sci. Eng. C 2017, 77, 1349–1362.

55. Zahedi, S.M.; Mansourpanah, Y. Construction of chitosan-carboxymethyl beta-cyclodextrin silver nanocomposite hydro gel to improve antibacterial activity. Plast. Rubber Compos. 2018, 47, 273–281.

56. Liu, L.; Wen, H.; Rao, Z.; Zhu, C.; Liu, M.; Min, L.; Fan, L.; Tao, S. Preparation and characterization of chitosan–collage n peptide/oxidized konjac glucomannan hydrogel. Int. J. Biol. Macromol. 2018, 108, 376–382.

57. Qin, D.; Zhang, A.; Wang, N.; Yao, Y.; Chen, X.; Liu, Y. Hydroxybutyl chitosan/ oxidized glucomannan self-healing hydro gels as BMSCs-derived exosomes carriers for advanced stretchable wounds. Appl. Mater. Today 2022, 26, 101342.

58. Jiang, Y.; Li, G.; Liu, J.; Li, M.; Li, Q.; Tang, K. Gelatin/Oxidized Konjac Glucomannan Composite Hydrogels with High R esistance to Large Deformation for Tissue Engineering Applications. ACS Appl. Bio Mater. 2021, 4, 1536–1543.

59. Wu, H.; Bu, N.; Chen, J.; Chen, Y.; Sun, R.; Wu, C.; Pang, J. Construction of Konjac Glucomannan/Oxidized Hyaluronic Acid Hydrogels for Controlled Drug Release. Polymers 2022, 14, 927.

60. Chen, H.; Lan, G.; Ran, L.; Xiao, Y.; Yu, K.; Lu, B.; Dai, F.; Wu, D.; Lu, F. A novel wound dressing based on a Konjac gl ucomannan/silver nanoparticle composite sponge effectively kills bacteria and accelerates wound healing. Carbohydr. Polym. 2018, 183, 70–80.

61. Ribeiro, J.S.; Bordini, E.A.F.; Ferreira, J.A.; Mei, L.; Dubey, N.; Fenno, J.C.; Piva, E.; Lund, R.G.; Schwendeman, A.; Bo ttino, M.C. Injectable MMP-Responsive Nanotube-Modified Gelatin Hydrogel for Dental Infection Ablation. ACS Appl. M ater. Interfaces 2020, 12, 16006–16017.

62. Pal, S.; Tak, Y.K.; Song, J.M. Does the Antibacterial Activity of Silver Nanoparticles Depend on the Shape of the Nanop article? A Study of the Gram-Negative Bacterium Escherichia coli. Appl. Environ. Microbiol. 2007, 73, 1712–1720.

63. Huang, T.; Xu, X.-H.N. Synthesis and characterization of tunable rainbow colored colloidal silver nanoparticles using sin gle-nanoparticle plasmonic microscopy and spectroscopy. J. Mater. Chem. 2010, 20, 9867–9876.

64. de Lacerda Coriolano, D.; de Souza, J.B.; Bueno, E.V.; Medeiros, S.; Cavalcanti, I.D.L.; Cavalcanti, I.M.F. Antibacterial and antibiofilm potential of silver nanoparticles against antibiotic-sensitive and multidrug-resistant Pseudomonas aerugi nosa strains. Braz. J. Microbiol. 2021, 52, 267–278.

65. Paladini, F.; Pollini, M. Antimicrobial Silver Nanoparticles for Wound Healing Application: Progress and Future Trends. Materials 2019, 12, 2540.

66. Wang, Q.; Qiu, W.; Li, M.; Li, N.; Li, X.; Qin, X.; Wang, X.; Yu, J.; Li, F.; Huang, L.; et al. Multifunctional hydrogel platform for biofilm scavenging and O2 generating with photothermal effect on diabetic chronic wound healing. J. Colloid Interface Sci. 2022, 617, 542–556.
67. Haidari, S.; FFA, I.J.; Metsemakers, W.J.; Maarse, W.; Vogely, H.C.; Ramsden, A.J.; McNally, M.A.; Govaert, G.A.M. The Role of Negative-Pressure Wound Therapy in Patients with Fracture-Related Infection: A Systematic Review and Critical Appraisal. BioMed Res. Int. 2021, 2021, 7742227.
68. Imran, M.; Hussain, S.; Mehmood, K.; Saeed, Z.; Parvaiz, M.; Younas, U.; Nadeem, H.A.; Ghalani, S.P.; Saleem, S. Optimization of ecofriendly synthesis of Ag nanoparticles by Linum usitatissimum hydrogel using response surface methodology and its biological applications. Mater. Today Commun. 2021, 29, 102789.
69. Alfuraydi, R.T.; Alminderej, F.M.; Mohamed, N.A. Evaluation of Antimicrobial and Antibiofilm Formation Activities of Novel Poly(vinyl alcohol) Hydrogels Reinforced with Crosslinked Chitosan and Silver Nano-Particles. Polymers 2022, 14, 1619.
70. Pérez-Díaz, M.; Alvarado-Gomez, E.; Magaña-Aquino, M.; Sánchez-Sánchez, R.; Velasquillo, C.; Gonzalez, C.; Ganem-Rondero, A.; Martínez-Castañon, G.; Zavala-Alonso, N.; Martinez-Gutierrez, F. Antibiofilm activity of chitosan gels formulated with silver nanoparticles and their cytotoxic effect on human fibroblasts. Mater. Sci. Eng. C Mater. Biol. Appl. 2016, 60, 317–323.
71. Katas, H.; Mohd Akhmar, M.A.; Suleman Ismail Abdalla, S. Biosynthesized silver nanoparticles loaded in gelatine hydrogel for a natural antibacterial and antibiofilm wound dressing. J. Bioact. Compat. Polym. 2021, 36, 111–123.
72. Vazquez-Muñoz, R.; Meza-Villezcas, A.; Fournier, P.G.J.; Soria-Castro, E.; Juarez-Moreno, K.; Gallego-Hernández, A.L.; Bogdanchikova, N.; Vazquez-Duhalt, R.; Huerta-Saquero, A. Enhancement of antibiotics antimicrobial activity due to the silver nanoparticles impact on the cell membrane. PLoS ONE 2019, 14, e0224904.
73. Li, X.; Li, B.; Liu, R.; Dong, Y.; Zhao, Y.; Wu, Y. Development of pH-responsive nanocomposites with remarkably synergistic antibiofilm activities based on ultrasmall silver nanoparticles in combination with aminoglycoside antibiotics. Colloids Surf. B Biointerfaces 2021, 208, 112112.
74. Lopez-Carrizales, M.; Mendoza-Mendoza, E.; Peralta-Rodriguez, R.D.; Pérez-Díaz, M.A.; Portales-Pérez, D.; Magaña-Aquino, M.; Aragón-Piña, A.; Infante-Martínez, R.; Barriga-Castro, E.D.; Sánchez-Sánchez, R.; et al. Characterization, antibiofilm and biocompatibility properties of chitosan hydrogels loaded with silver nanoparticles and ampicillin: An alternative protection to central venous catheters. Colloids Surf. B Biointerfaces 2020, 196, 111292.
75. Wunnoo, S.; Bilhman, S.; Waen-ngoen, T.; Yawaraya, S.; Paosen, S.; Lethongkam, S.; Kaewnopparat, N.; Voravuthikunchai, S.P. Thermosensitive hydrogel loaded with biosynthesized silver nanoparticles using Eucalyptus camaldulensis leaf extract as an alternative treatment for microbial biofilms and persistent cells in tissue infections. J. Drug Deliv. Sci. Technol. 2022, 74, 103588.